

# Linking Giant Molybdenum Oxide Based Nano-Objects Based on Well-Defined Surfaces in Different Phases

Achim Müller\*<sup>[a]</sup> and Soumyajit Roy<sup>[a]</sup>

**Keywords:** Films / Hydrophilic surfaces / Monolayers / Nanochemistry / Polyoxomolybdates / Surfactant-encapsulated clusters / Surface structures / Vesicles

The linking of nanosized clusters is especially interesting if the following conditions are fulfilled: The nano-objects, as in the present case, have interesting properties like *well-defined* functionalized external and internal surfaces, linking processes follow *well-defined* rules and occur with respect to formation of discrete as well as extended structures under mild conditions in different phases, i.e. in the gas, solution and solid phase. In the present microreview it is shown that

the wheel- and sphere-shaped nanosized molybdenum-oxide based clusters fulfil these conditions while extensive linking is observed even under one-pot conditions, which means that the clusters primarily formed by self-assembly can become further linked in the same phase.

(© Wiley-VCH Verlag GmbH & Co. KGaA, 69451 Weinheim, Germany, 2005)

The chemistry of varying connectivity is a fascinating subject. Nature has long made use of this phenomenon as a means to induce structural diversity. From dazzling diamonds to charry coals, from liquid aniline to its conducting plastic polymer,<sup>[1]</sup> the varying fluidity of the membranes,<sup>[2a]</sup>

from a basic building unit to a variety of supramolecular structures,<sup>[2b–2f]</sup> from crystalline quartz to ornate shells of diatoms and related bio- (or bio-mimetic) architectures,<sup>[2g–2k]</sup> are but only a few illustrations of varying connectivity. The underlying principle in all cases is nearly the same, varied but iterative linking of basic building blocks. The tale becomes especially interesting from a chemist's point of view if the above principle can be deliberately realized in a reaction system which has the intrinsic potential to show connectivity variability under different conditions,

[a] Lehrstuhl für Anorganische Chemie I, Fakultät für Chemie der Universität, Postfach 100131, 33501 Bielefeld, Germany  
Fax: +49-521-106-6003  
E-mail: a.mueller@uni-bielefeld.de



Achim Müller (left) studied chemistry and physics at the University of Göttingen and received his Ph.D. (1965) and his Habilitation (1967) there. In 1971, he became professor at the University of Dortmund (Germany), and in 1977 accepted the chair of Inorganic Chemistry at the University of Bielefeld, where he is still Professor of the Faculty of Chemistry. His research involves the chemistry of transition metals, particularly inorganic supramolecular chemistry and bioinorganic chemistry in synthesis, spectroscopy, and theory. He has published, besides numerous original papers, more than 35 reviews and is coeditor of several books, including "The Chemistry of Nanomaterials" with C. N. R. Rao and A. K. Cheetham in 2004 (Wiley-VCH). The latest of his very many national and international awards in 2005 are an honorary doctorate of the University Pierre et Marie Curie (Paris) and an award, the Premio Elhuyar Goldschmidt, of the Real Sociedad Española de Química (RSEQ, Spanish Chemical Society). He also delivered this year's annual Lewis Lecture at the University of Cambridge.

S. Roy (right) obtained his M. Sc from the Indian Institute of Technology, Delhi, India, and has just completed his doctoral dissertation under the supervision of Prof. A. Müller at the University of Bielefeld.



**MICROREVIEWS:** This feature introduces the readers to the authors' research through a concise overview of the selected topic. Reference to important work from others in the field is included.

e.g. in the gas phase, in solution or under solid-state conditions. The solutions of oxoanions of the early transition metals, in particular the polyoxomolybdates under reducing conditions considered here, provide spectacular possibilities to explore the enormous connectivity variety that can be achieved by linking together metal-oxide based building blocks or even the resulting nanosized clusters.<sup>[3]</sup> Examples include spherical nanocapsules with unique receptor properties like those of the  $\{\text{Mo}_{132}\}$  Keplerate type,<sup>[4]</sup> the giant wheel-type cluster anions like  $\{\text{Mo}_{154}\}$ ,<sup>[5]</sup> and the “blue lemon”  $\{\text{Mo}_{368}\}$ -type species<sup>[6]</sup> (all formed from metal-oxide fragments as building blocks) as well as the formation of chains or layers from these clusters which themselves act as building blocks. In this microreview an account of such covalent structuring in the solid state leading to periodicity is depicted as a concluding section and is preceded by different types of “super-structuring” in the gas phase, in solution and on surfaces. The unprecedented linking versatility to be illustrated shortly is a consequence not only of the uniformly nanoscaled structured surfaces but especially of the characteristic/unique functionalizations [with the option for an interesting type of “scale chemistry, in which the size of the “secondary building blocks” (SBUs) in a structure is increased while maintaining the same connectivity between them [...]” (see ref.<sup>[7]</sup>)]. With respect to the structural variety of nanosized discrete species, the other polyoxometalates like the polyoxotungstates behave completely different from the polyoxomolybdates, i.e. they do not show the versatility of nanosized structures.

## 1. Structuring in the Gas Phase

“Uncharged” molybdenum-oxide giant spheres with a molecular mass of about 16 kDa can be “kicked out” like soccer balls into the gas phase using matrix-assisted laser desorption and ionization (MALDI) and be detected by time of flight (TOF) mass spectrometry.<sup>[8]</sup> These findings confirmed the existence of such giant clusters in the gas phase and opened a wide range of nontrivial experiments, i.e. single-molecule spectroscopy of nano-objects or the epitaxial growth of functionalized supramolecular layers or cluster collectives suitable for electronic devices (quantum-dot cellular automata). The practically neutral spherical clusters studied here, for the aforementioned related investigations, cocrystallized in a matrix of DCTB (2-[(2*E*)-3-(4-*tert*-butylphenyl)-2-methylprop-2-enylidene]malononitrile).

MALDI spectra for two spherical species of the type  $\{(\text{Mo})\text{Mo}_5\}_{12}\{\text{M}_{30}\}$  in the DCTB matrix were obtained. As main products, single spheres of the types  $\{\text{Mo}_{72}\{\text{Fe}_{30}(\text{Mo})_6\}$  (molecular mass 15.93 kDa with nearly all decorations, but without the crystal water),  $\{\text{Mo}_{72}\}\{\text{Mo}_{30}\}$  (15.94 kDa) singly and doubly charged, and remarkably, also oligomers with 2, 3, 4 and 5 spheres, again singly and doubly charged, were found. Taking into account the molecular mass of DCTB (250 Da), the mass distribution over the peaks covers the complete range from the fully ligand decorated (together with only a few matrix molecules) to the completely undecorated giant spheres (Figure 1).

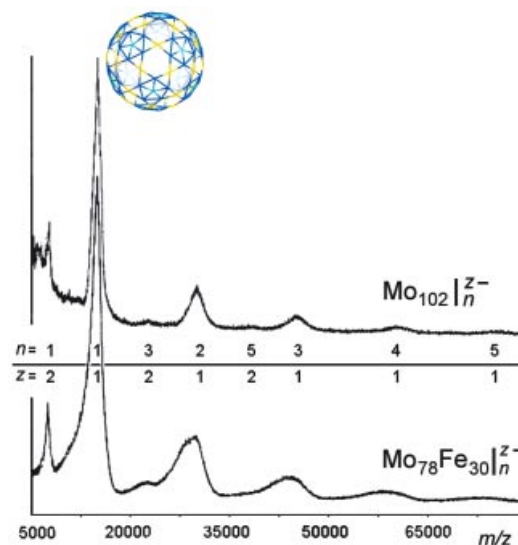


Figure 1. MALDI TOF mass spectra of the  $\{(\text{Mo})\text{Mo}_5\}\{\text{M}_{30}\}$ -type species ( $\text{M} = \text{Fe}, \text{Mo}$ ) and their oligomers (for details see ref.<sup>[8]</sup>).

## 2. Super Structuring in Solution

An interesting cluster connectivity was accomplished with super-structuring, and highlighted also as “rounding up”<sup>[9]</sup> of a huge number of  $\{\text{Mo}_{154}\}$ -type nanowheels in aqueous solution to vesicular nanoassemblies, i.e. to an inorganic skinned drop of water (for details on the topic not mentioned here, see ref.<sup>[10]</sup>).

The  $\{\text{Mo}_{154}\}$  based vesicles, almost monodisperse, were characterized by light-scattering data (DLS and SLS) as well as transmission and scanning electron microscopy, which revealed spherical hollow structures with an average, hydrodynamic radius of about 45 nm and comprising approximately  $12 \times 10^2$   $\{\text{Mo}_{154}\}$  wheel-shaped clusters (Figure 2). The clusters appear to lie flat and homogeneously distributed on the vesicle surface. A question may arise as to whether those entities are really hollow and not solid. It can be shown that they are, apart from the solvent inside.<sup>[11]</sup>

The unique/unprecedented phenomenon of self-assembling  $\{\text{Mo}_{154}\}$ -type nano-objects into a spherical vesicle is still not completely understood. However, it is expected that here the counter cations  $\text{Na}^+$ ,  $\text{H}^+$  and especially the different types of confined structured water play, besides attracting van der Waals forces, a crucial role in the story of vesicular stabilization. (The aqueous solution of the clusters is a medium strong acid, even “dissolving” metals like Zn.) Assuming that all the nanowheels are distributed on the surface in almost hexagonal closest packing, the center-to-center distance between two adjacent nanowheels would be around 4.9 nm, whereas the diameter of an individual nanowheel is according to X-ray crystallography 3.6 nm. This infers that the nanowheels are not touching each other on the vesicle surface.

As mentioned above, water assemblies and counter cations are expected to play an important role in filling gaps and holding the overall assemblies together, while the struc-

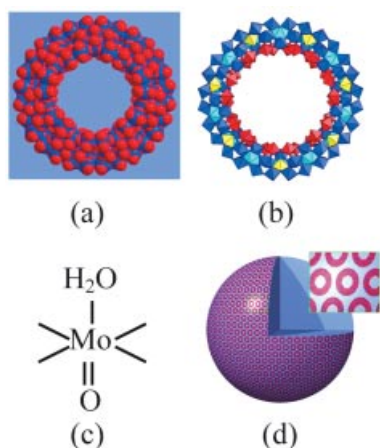


Figure 2. Structure of the 3.6 nm size  $\{\text{Mo}_{154}\}$ -type nanowheel with a hydrophilic surface and nanosized central cavity as well as the related vesicle. (a) Space-filling representation (Mo atoms blue and light blue; O atoms red). (b) Polyhedral representation, demonstrating the abundance of pentagonal  $\{(\text{Mo})\text{Mo}_5\}$  units (in blue) probably influencing the water structure ( $\{\text{Mo}_2\}$  units red;  $\{\text{Mo}_1\}$  units yellow). (c) The typical smallest fragment with a metal atom and its coordination sphere, i.e., with one of the 70  $\text{H}_2\text{O}$  ligands causing the extreme hydrophilic nature that is responsible for the interaction with solvents such as water. (d) Schematic plot of the vesicle structure ( $\approx 45$  nm radius) formed from ca.  $12 \times 10^2$  nanowheels in aqueous solution; the inset shows enlarged nanowheels.

tured water would in a way especially explain the stability of the vesicles! Indeed, the integration of a large number of nano-objects on an ordered spherical surface seems to be highly *anti*-entropic and hence a highly unlikely event (Figure 2). But the release of some of the “local” strongly hydrogen bonded water molecules from the vicinity of the clusters to the “bulk” water pays the high price for the mentioned entropy decrease.

These results are also interesting as the molecular  $\{\text{Mo}_{154}\}$ -type wheels show, because of the abundance of 70 coordinated  $\text{H}_2\text{O}$  ligands, an extremely hydrophilic surface causing a well-defined hydration shell. This again causes extreme solubility, which for more than 200 years prevented chemists from the time of Scheele and Berzelius who performed the first related experiments, from isolating them in a crystalline state.<sup>[12a]</sup> Now it can be shown by dielectric relaxation studies<sup>[12b]</sup> that there are different kinds of confined water in and on these systems; for instance the water inside the wheel-type cavity is more strongly fixed (thus less mobile) than the water at the surface, while both are probably involved in the stabilization of the vesicles. This correlates with the above-mentioned hydrophilicity and especially the strong cluster surface water interaction.

### 3. Encapsulation by Surfactants and Surface Structuring: Films and Monolayers

The motivation to examine “Surfactant Encapsulated Clusters” (SECs) rather than only “naked” ones had the following base: the surfactant shell improves the *stability* of the encapsulated cluster against *fragmentation*, enhances

the *solubility* in nonpolar, aprotic organic solvents, neutralizes their *charge*, thus leading to discrete, *electrostatically neutral* assemblies, while altering the *surface chemical properties* (e.g. self-aggregation, surface adhesion, wetting behavior) in a predictable manner. Some related investigations<sup>[13,14]</sup> are reviewed here, also deliberately with respect to some details.

The discrete hybrid  $(\text{DODA})_{40}(\text{NH}_4)_2[(\text{H}_2\text{O})_n\text{C}\text{Mo}_{132}\text{O}_{372}(\text{CH}_3\text{COO})_{30}(\text{H}_2\text{O})_{72}]$  ( $n \approx 50$ ) for example is formed by spontaneous self-assembly (see Figure 3). It consists of a hollow giant spherical isopolyoxomolybdate core covered by a hydrophobic shell of dimethyldioctadecylammonium

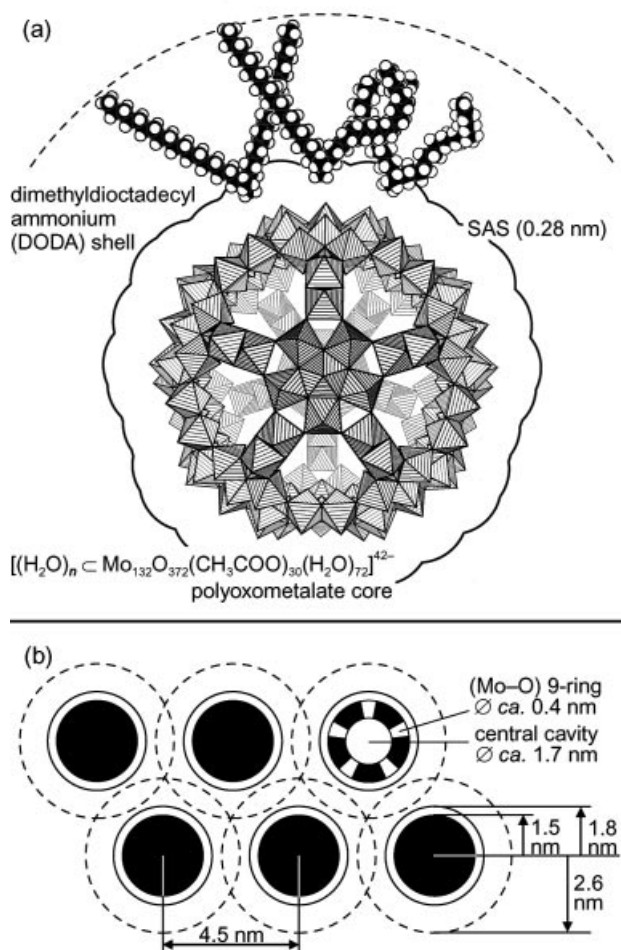


Figure 3. (a) Schematic representation of the surfactant-encapsulated cluster (SEC). The Mo–O framework of the  $\{\text{Mo}_{132}\}$ -type cluster is shown in polyhedral representation. The DODA amphiphiles, only a fraction of which are represented in the Scheme, form a hydrophobic shell around the cluster. Molecular dynamics simulations of a single SEC placed within a periodic solvent-filled ( $\text{CHCl}_3$ ) box indicate that in solution the relative density of the appending  $\text{C}_{18}$  chains decreases as the radial distance from the cluster increases. Due to the conformational flexibility of the  $\text{C}_{18}$  chains, the external boundary of the SEC (represented by the broken line) is not sharply defined. (b) Schematic representation of a single SEC layer according to TEM data and molecular models. The SECs arrange on a 2D lattice to form a closest packing. Surfactant shells of neighboring SECs locally interpenetrate one another. One of the SECs is displayed cross-sectioned to further highlight the supramolecular architecture.



(DODA) cations, which was the basis for the generation of well-defined films and monolayers.<sup>[13]</sup> The structural characterization of the nanoporous core-shell particles was based on small-angle X-ray scattering (SAXS) data (on solutions of the encapsulated clusters), transmission electron microscopy (TEM) investigations, FT-IR and UV/Vis spectroscopy, as well as the determination of the molecular area of the encapsulated cluster by Langmuir–Blodgett (LB) film investigations.<sup>[13]</sup> Computer modeling of the solvent-accessible surface of the encapsulated cluster yielded a central cavity with a volume of  $1.5(\pm 0.3) \text{ nm}^3$ . The cavity is occupied by approximately  $50(\pm 15) \text{ H}_2\text{O}$  molecules, which are, in the case of the present acetate system with a hydrophobic shell interior, not densely packed. The covered surface area of  $84 \text{ Å}^2/\text{DODA}$  indicates a rather tight packing of the amphiphiles at the cluster/capsule surface.

The discrete cluster hybrids have been directly imaged by transmission electron microscopy.<sup>[13]</sup> Figure 4a shows a thin film originally cast onto a water surface. The inorganic cores of  $(\text{DODA})_{40}(\text{NH}_4)_2[(\text{H}_2\text{O})_n\text{C Mo}_{132}\text{O}_{372}(\text{CH}_3\text{COO})_{30}(\text{H}_2\text{O})_{72}]$  ( $n \approx 50$ ) appear as dark spots embedded in a bright matrix of surfactant molecules. Both the diameter of the dark objects (ca. 3 nm), as well as the average distance between them (ca. 4.5 nm), match the film structure depicted in Figure 4b. The image shows monolayer regions, regions consisting of a bilayer (darker) and the uncovered substrate (brighter), while small domains exhibit hexagonal arrays of SECs corresponding to a two-dimensional dense packing of spherical particles (arrows). The order improves in thicker films and becomes three-dimensional. An ordered region is shown in Figure 4b; the related electron diffraction pattern (insert) clearly reveals long-range order (spots rather than rings) and a threefold symmetry for the pattern of reflections corresponding to a spacing of 4.2 nm. In accordance with the presence of local fourfold symmetry projections it can be assumed that the SECs are arranged on a fcc lattice with the most dense (111) planes preferentially oriented parallel to the substrate, as is the case of latex films. It may therefore be concluded that the diffraction pattern reflects the structure from the triangular array of particles in a (111) plane at normal orientation to the beam, and that the packing of the SECs is best described within a fcc lattice with a cubic unit-cell axis of approximately 6 nm.

A characteristic feature of the present type of SEC is that it spreads at the air–water interface. This property was used to measure its molecular area. From the compression isotherm of a monolayer of the cluster (Figure 5), a molecular area of  $15 \text{ nm}^2$  at the collapse point could be determined, which corresponds to the densest possible packing. Based on the assumption of a void-free monolayer in which the inorganic cluster cores are packed in a hexagonal array (Figure 3b), a core-to-core distance of 4.2 nm was obtained, a result that is in excellent agreement with the TEM data. The molecular area for noninteracting SECs determined at the onset of the isotherm ( $\pi = 0$ ) is  $32 \text{ nm}^2$ , which corresponds to a diameter (of the spherical projection) of 6.4 nm.

Due to the unique supramolecular architecture of the surfactant encapsulated cluster (SEC) as well as its high sol-

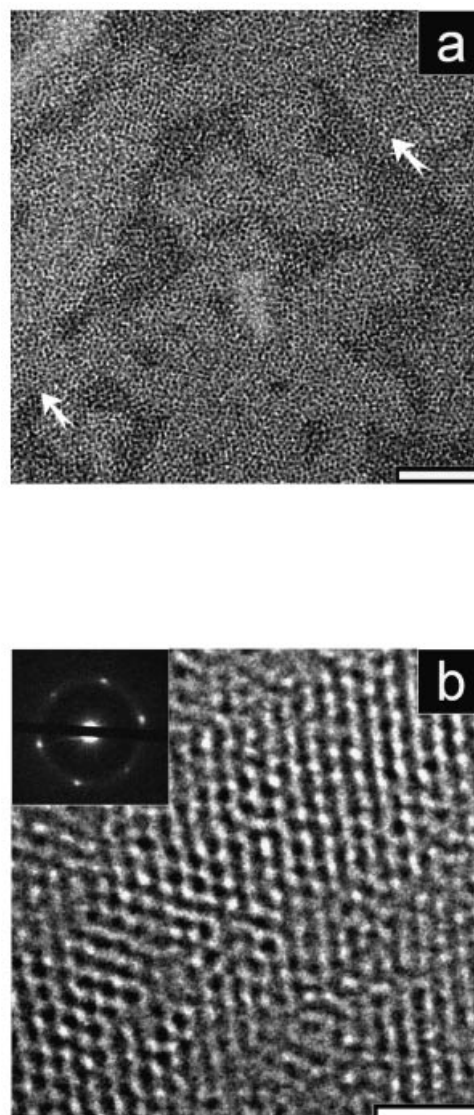


Figure 4. Shown is (a) a TEM micrograph of a thin film of SECs (scale bar 50 nm). Extended monolayers, interspersed with holes and doublelayer regions, are clearly visible (two arrows mark some regions of apparent hexagonal order). (b) TEM micrograph of an ordered region of a thicker film at high magnification (scale bar 20 nm). The insert shows a low-angle electron diffraction pattern (elastically filtered) recorded from a larger area ( $5 \mu\text{m}^2$ ) containing the region shown.

ubility in common organic solvents, this aggregate shows promising perspectives for future applications in host–guest chemistry and homogeneous size-selective catalysis.

#### 4. Extended Structuring in the Solid State

Controlled assembly of building blocks by *specific linking* in a self-assembly process following an “Aufbau” principle leading to the metal-oxide based nanoscaled clusters as mentioned above, inevitably comes up with an imminent question. Is it possible to use those self-assembled structures as “secondary building blocks” to generate even “*extended*” complex topologies by “*extended*” linking? In our

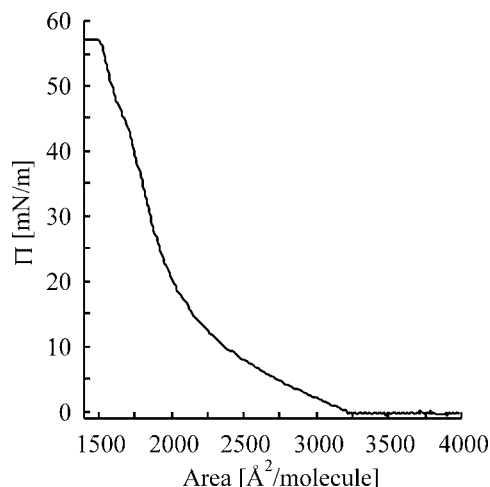


Figure 5. Surface pressure-area ( $\pi - A$ ) isotherm of the SEC at the air-water interface.

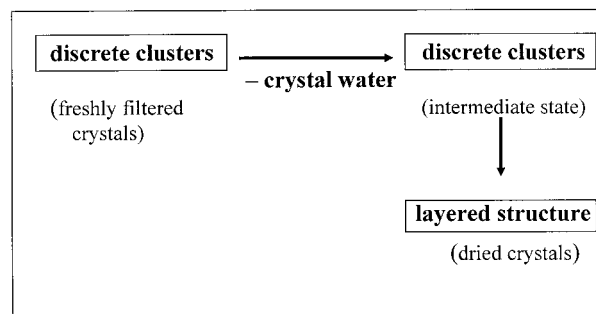
case the question was whether it is possible to “trigger” a special aggregation-type process to extensively link [(pentagon)<sub>12</sub>(linker)<sub>30</sub>]-type species and/or the circular {Mo<sub>154</sub>}-type nano-objects, as “secondary building blocks”. In fact it was possible to find an easy solution to the problem. A simple condensation-type reaction with the loss of water molecules solves the problem by triggering a self-organization type process even under solid-state conditions at room temperature, thereby getting the primarily formed parent-type nano-objects linked in the same phase. In the following Section we will discuss five prototypal cases of such processes, which elegantly demonstrate the basic principles of “scale chemistry”<sup>[7a]</sup> in the context of connectivity.

#### 4.1 Cross-Linking the [(Mo)Mo<sub>5</sub>]<sub>12</sub>{Fe}<sub>30</sub>]-Type Capsules According to Their Acidic Properties to 2D Layers: A Remarkable Room-Temperature Solid-State Reaction

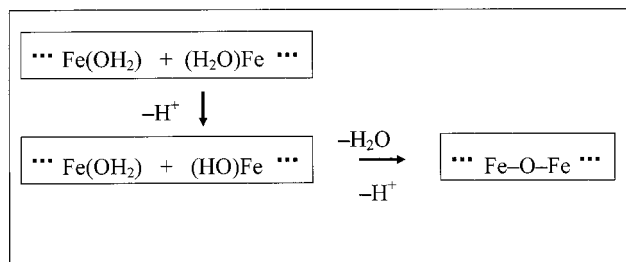
A well-known reaction in inorganic chemistry is a condensation process in aqueous solution between acidic [M<sup>III</sup>(H<sub>2</sub>O)<sub>6</sub>]<sup>3+</sup>-type complexes with the resulting loss of protons and water that leads to the formation of iron polycations via M–O–M linkages.<sup>[15]</sup> Such a reaction has a very low activation energy and hence could in principle proceed in the present [(Mo)Mo<sub>5</sub>]<sub>12</sub>{Fe}<sub>30</sub>-type capsule situation because of the abundance of 30 [Fe(H<sub>2</sub>O)<sub>2</sub>]<sup>3+</sup> groups as linkers.<sup>[16a]</sup>

Correspondingly, it was in fact observed that even in a room-temperature solid-state reaction the [(Mo)Mo<sub>5</sub>]<sub>12</sub>{Fe}<sub>30</sub>-type nano-objects become cross-linked.<sup>[16b,16c]</sup> The rapid loss of loosely bound crystal water molecules leads to a situation where the discrete spherical clusters are abundant in the compound [(Mo)Mo<sub>5</sub>]<sub>12</sub>Fe<sub>30</sub>O<sub>252</sub>(CH<sub>3</sub>COO)<sub>12</sub>{Mo<sub>2</sub>O<sub>7</sub>(H<sub>2</sub>O)}<sub>2</sub>{H<sub>2</sub>Mo<sub>2</sub>O<sub>8</sub>(H<sub>2</sub>O)}(H<sub>2</sub>O)<sub>91</sub>·ca. 150 H<sub>2</sub>O, i.e. the corresponding freshly filtered monoclinic crystals can come into contact, which is a condition for the interaction. This finally leads to the formation of [H<sub>4</sub>Mo<sub>72</sub>Fe<sub>30</sub>O<sub>254</sub>(CH<sub>3</sub>COO)<sub>10</sub>{Mo<sub>2</sub>O<sub>7</sub>(H<sub>2</sub>O)}{H<sub>2</sub>Mo<sub>2</sub>O<sub>8</sub>(H<sub>2</sub>O)}(H<sub>2</sub>O)<sub>87</sub>·ca. 80 H<sub>2</sub>O, with a layered structure forming platelike crystals (see Schemes 1 and 2 and Figure 6). It is assumed that the finally released H<sup>+</sup> ions protonate the spherical cluster units. (Note: [(Mo)Mo<sub>5</sub>]<sub>12</sub>{Fe}<sub>30</sub>-type clusters can also be obtained as discrete entities in rhombohedral crystals, where the reaction does not proceed, probably because of a different type of packing.) The (nearly) electrical neutrality of the cluster units facilitates the easy loss of water and hence cross-linking. The reaction steps (see Scheme 1 and Scheme 2) involved in cross-linking clearly show as expected a decrease in the volume of the unit cell.

O<sub>8</sub>(H<sub>2</sub>O)<sub>3</sub>(H<sub>2</sub>O)<sub>87</sub>·ca. 80 H<sub>2</sub>O, with a layered structure forming platelike crystals (see Schemes 1 and 2 and Figure 6). It is assumed that the finally released H<sup>+</sup> ions protonate the spherical cluster units. (Note: [(Mo)Mo<sub>5</sub>]<sub>12</sub>{Fe}<sub>30</sub>-type clusters can also be obtained as discrete entities in rhombohedral crystals, where the reaction does not proceed, probably because of a different type of packing.) The (nearly) electrical neutrality of the cluster units facilitates the easy loss of water and hence cross-linking. The reaction steps (see Scheme 1 and Scheme 2) involved in cross-linking clearly show as expected a decrease in the volume of the unit cell.



Scheme 1.



Scheme 2.

#### 4.2 “Necklace”-Type Linking of Spherical Capsules

From two-dimensional layers to a one-dimensional chain or necklace, a transition, which might initially seem problematic but, which in fact, follows the same thread of chemical logic. The formation of one-dimensional chains of related similar nano-objects involves, in principle, a reaction of the same type, which is based on a compound containing (nearly neutral) discrete [(Mo<sup>VI</sup>)Mo<sup>VI</sup><sub>5</sub>]<sub>12</sub>{Mo<sup>V</sup><sub>6</sub>Fe<sup>III</sup><sub>24</sub>}- (CH<sub>3</sub>COO)<sub>20</sub>O<sub>258</sub>(H<sub>2</sub>O)<sub>84</sub>]<sup>2-</sup> clusters. When the black crystals containing the mentioned clusters are dried, the latter becomes linked to form one-dimensional chains with the stoichiometry [(Mo<sup>VI</sup>)Mo<sup>VI</sup><sub>5</sub>]<sub>12</sub>{Mo<sup>V</sup><sub>6</sub>Fe<sup>III</sup><sub>24</sub>}- (CH<sub>3</sub>COO)<sub>20</sub>-O<sub>258</sub>(H<sub>2</sub>O)<sub>82</sub>]<sup>2-</sup>. The reaction is triggered by the rapid loss of crystal water molecules (Figure 7 and Figure 8),<sup>[17]</sup> which causes the obligatory decrease of inter-sphere distances and leads to the situation where an Mo=O group of one discrete sphere can formally act as a ligand while replacing H<sub>2</sub>O groups attached to Fe<sup>III</sup> centers of an adjacent sphere in an

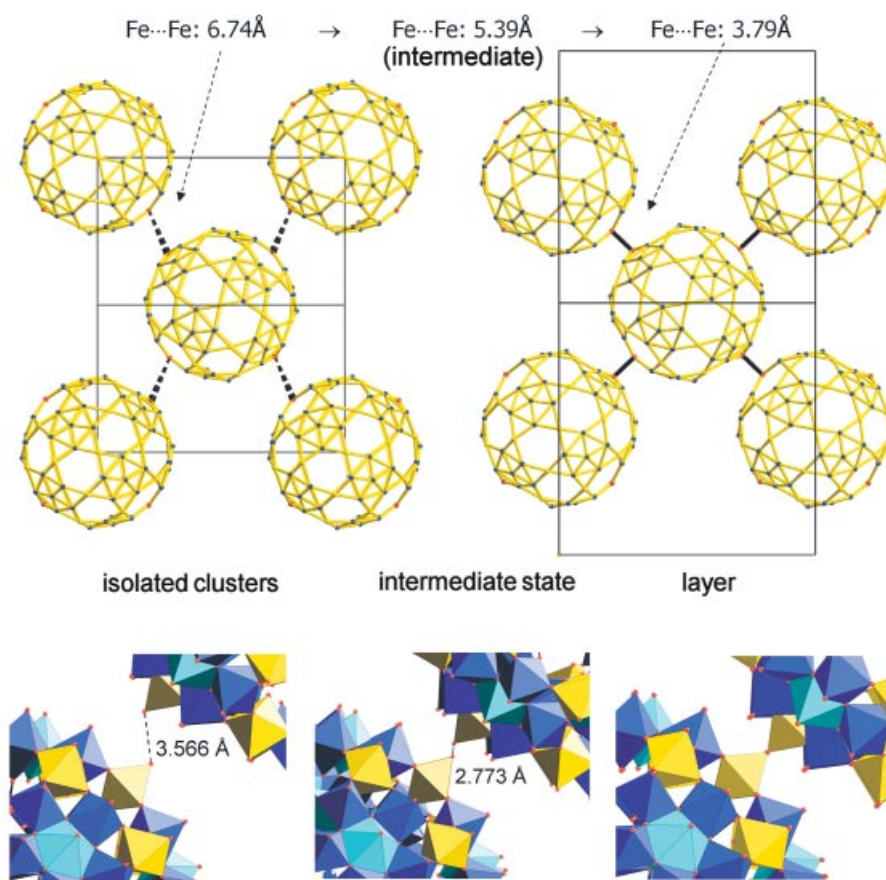


Figure 6. Wireframe representation (in yellow/blue) of the metal skeleton of the  $\{\text{Mo}_{72}\text{Fe}_{30}\}$ -type cluster units indicating their covalent cross-linking to a layer structure (top right). The solid-state room-temperature conversion process leading to its formation takes place according to Scheme 1 and Scheme 2 given in the text. The reaction proceeds from discrete cluster units (top left) present in the wet monoclinic crystals, freshly filtered from the mother liquor, via an intermediate state (top middle) with discrete units positioned at the minimum possible distances without covalent bond formation to the final (rhombic) crystalline product. (Note: the same does not occur for rhombohedral crystals with discrete units.<sup>[16a]</sup>) The related segment demonstrating the linking is given in polyhedral representation ( $\text{Fe}_6$  yellow; Mo polyhedra blue).

$S_N$ -type reaction. It is important to note that this mechanism is much more complicated than that in the above-mentioned cross-linking case. It should further be noted that the present clusters due to their lower symmetry do not allow an easy further higher-symmetrical cross-linking, i.e. with two-dimensional periodicity.

In the present case and in that of the previous Section (4.1), it should in principle also be possible to form oligomers when the existing boundary conditions prevent extended linking.

#### 4.3 Cross-Linking of the Spherical Clusters Exhibiting Encapsulated “Guests”, i.e. Composites with Nucleus-Shell Topology

The chemistry of connectivity could become even more exciting if it is possible to “cross-link” not only empty spherical capsules like those described above, but also “host-guest”-type composites – especially those with unusual host-guest interactions – to a network. The above-mentioned experiments have shown that it is possible to

connect  $[(\text{Mo})\text{Mo}_5]_{12}[\text{Fe}]_{30}$ -type moieties, but the question arises, can such moieties, which are reacting to become linked, contain guests?

Interestingly, the cavities inside the (practically uncharged)  $[(\text{Mo})\text{Mo}_5]_{12}[\text{Fe}]_{30}$ -type clusters are large enough to host Keggin-type anions with a diameter of ca. 14 Å. The latter can be incorporated into the cavity of the former by merely adding them to a solution ambient to the generation of the host cluster shells.<sup>[18]</sup> The resulting molybdenum-oxide based “host-guest” composite with an encapsulated Keggin ion presents an unprecedented noncovalent, i.e. supramolecular host-guest interaction (Figure 9).<sup>[19]</sup> Here the Keggin ion (guest) can, in principle, also act as a “kind of template” for the generation of the host as it accelerates its formation.

It finally turned out that these “host-guest” supramolecular nanocomposites can be linked in a way that is identical to that of the empty spherical capsules to form layers (see Section 4.1). In other words, these host-guest nanocomposites also undergo a cross-linking type of solid-state condensation reaction at room temperature to form a layered net-



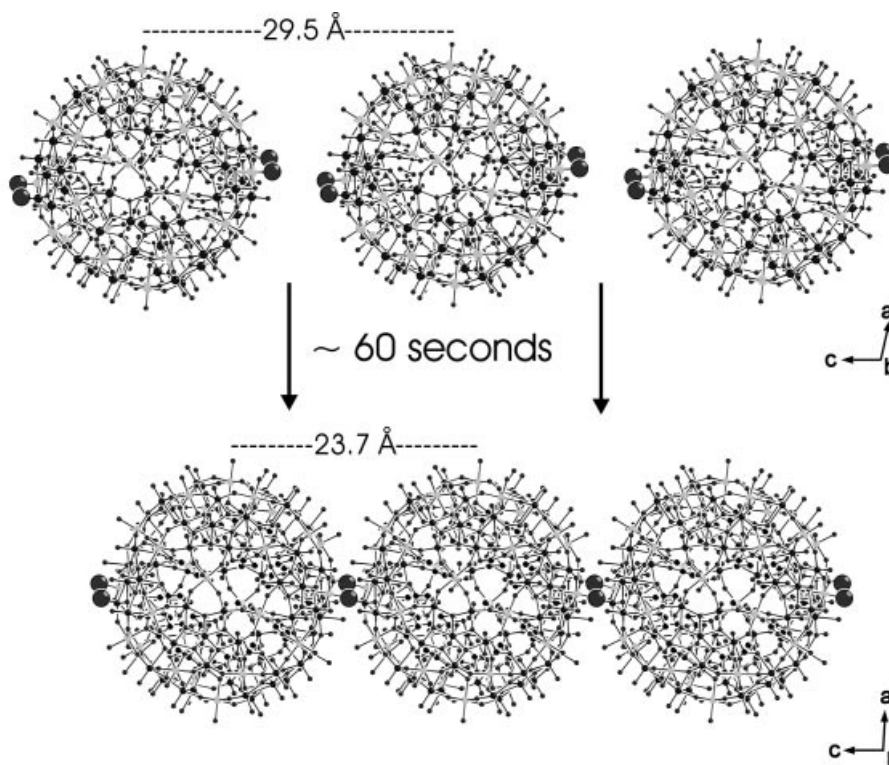


Figure 7. Schematic representation of the room-temperature solid-state reaction (see also Figure 8) leading to the formation of the chain (bottom) present in the compound  $\text{Na}_2[\{(\text{Mo}^{\text{VI}})\text{Mo}^{\text{VI}}_5\}_{12}\{\text{Mo}^{\text{V}}\text{Fe}^{\text{III}}_{24}\}(\text{CH}_3\text{COO})_{20}\text{O}_{258}(\text{H}_2\text{O})_{82}\}\cdot\text{ca. } 80 \text{ H}_2\text{O}$  caused by linking the discrete spheres  $[\{(\text{Mo}^{\text{VI}})\text{Mo}^{\text{VI}}_5\}_{12}\{\text{Mo}^{\text{V}}\text{Fe}^{\text{III}}_{24}\}(\text{CH}_3\text{COO})_{20}\text{O}_{258}(\text{H}_2\text{O})_{84}\}]^{2-}$  (top).<sup>[17]</sup> Note the (small) error limit in the number of  $\text{Mo}^{\text{V}}$  centers and the corresponding (possible) cluster charge.

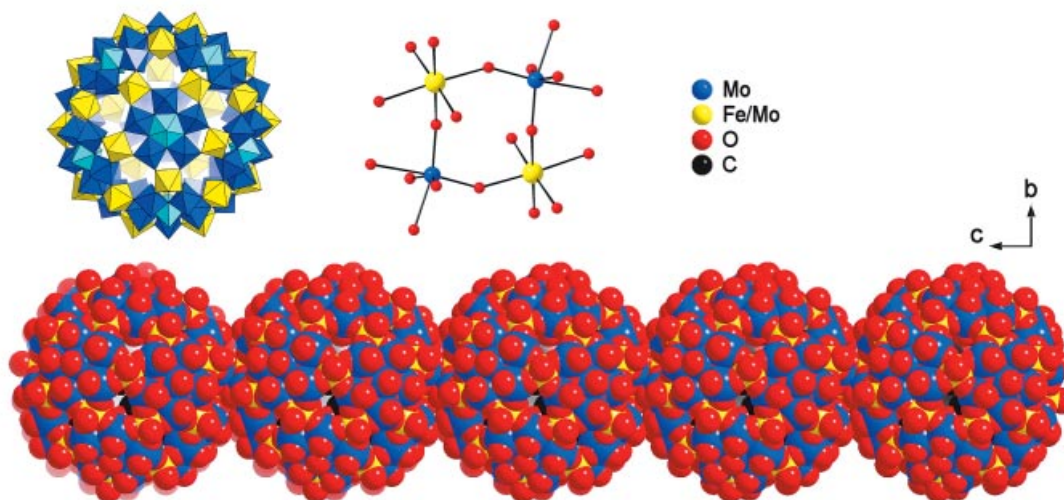


Figure 8. More detailed representation of the structures depicted in Figure 7 showing 1) the discrete anion (polyhedral representation, top left) in crystals of  $\text{Na}_2[\{(\text{Mo}^{\text{VI}})\text{Mo}^{\text{VI}}_5\}_{12}\{\text{Mo}^{\text{V}}\text{Fe}^{\text{III}}_{24}\}(\text{CH}_3\text{COO})_{20}\text{O}_{258}(\text{H}_2\text{O})_{84}\}\cdot\text{ca. } 150 \text{ H}_2\text{O}$ , and 2) the anionic chain (Figure 7) in these crystals (bottom, space-filling representation). The linking area is separately given in ball-and-stick representation (top right); bond lengths [Å] and angles [°] in the  $\text{M}_4\text{O}_4$  ( $\text{M} = \text{Mo}/\text{Fe}$ ) ring: Mo–O: 1.72/1.78; Fe–O: 1.96/1.98; Mo–O–Fe: 147.0/149.9; O–Mo–O: 101.5; O–Fe–O: 93.2.<sup>[17]</sup>

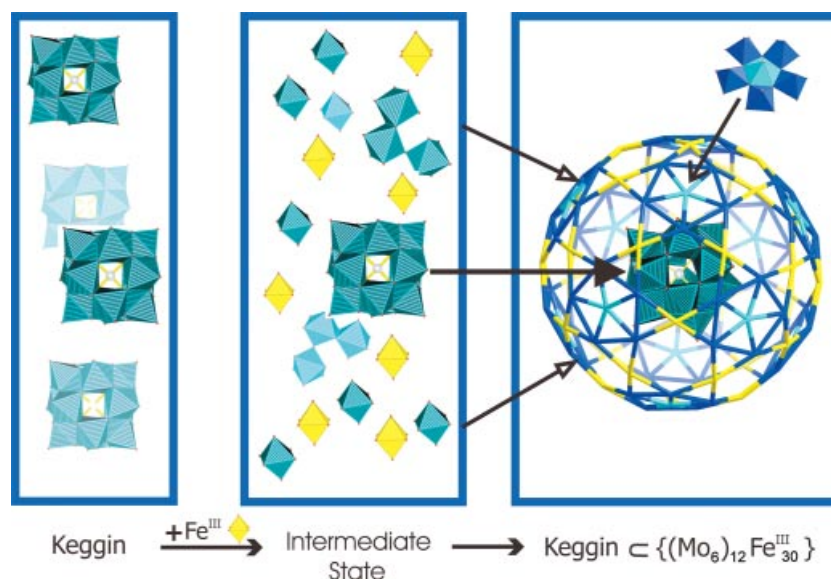


Figure 9. Reaction Scheme showing the decomposition of part of the Keggin anions  $\{\text{PMo}_{12}\text{O}_{40}\}^{3-}$  (left, polyhedral representation) in the presence of  $\text{Fe}^{3+}$  in aqueous solution, leading finally to the formation of the spherical  $\{(\text{Mo})\text{Mo}_5\}_{12}\{\text{Fe}\}_{30}$ -type cage [with wireframe representation of the capsule's Mo atoms (in cyan and dark blue) and Fe atoms (in yellow)] which has one of the remaining nondecomposed Keggin anions encapsulated (polyhedral representation) thus forming the unusual supramolecular species with core-shell topology: guest  $\subset [(\text{pentagon})_{12}(\text{linker})_{30}]$  ( $\text{FeO}_6$  octahedra yellow).

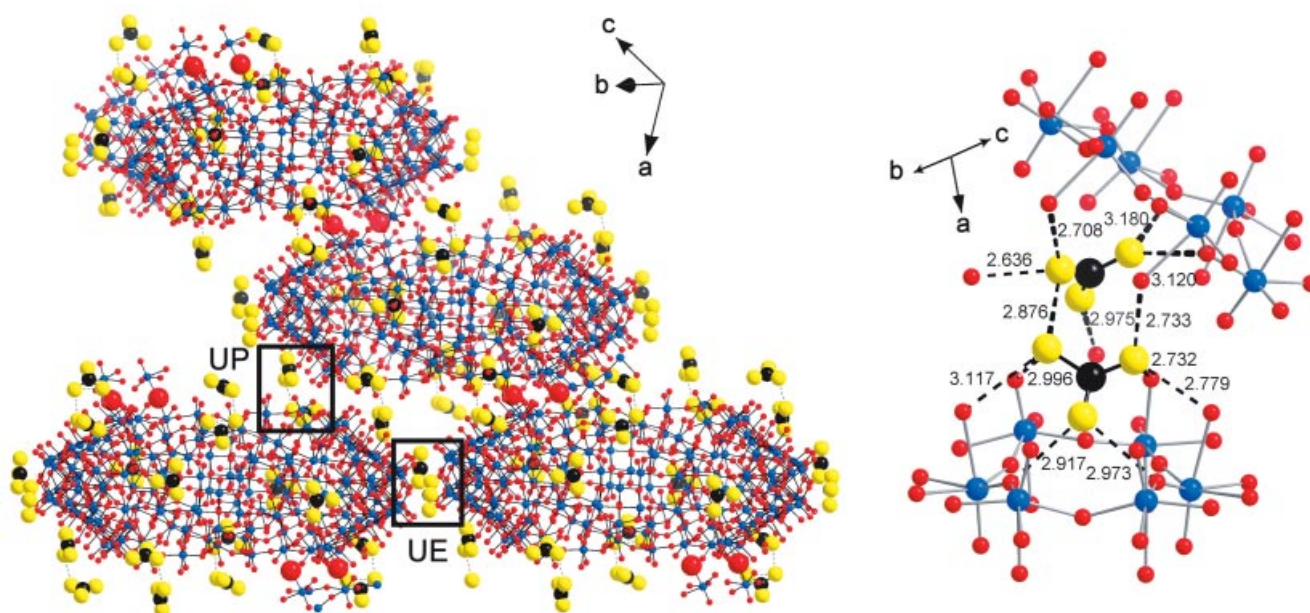


Figure 10. Left: ball-and-stick representation of four  $\{\text{Mo}_{154}\}$ -type rings of the compound  $\frac{1}{6}(\text{NH}_3\text{CONH}_2)_{14}[\text{Mo}^{\text{VI}}_{126}\text{Mo}^{\text{V}}_{28}\text{O}_{462}\text{H}_{14}(\text{H}_2\text{O})_{68}] \cdot \text{ca. } 350 \text{ H}_2\text{O}$  "glued" with two types of protonated urea molecules [viz., equatorial (UE) as well as polar (UP)]. The atoms of the urea (type) units and the oxygen atoms which covalently connect adjacent rings have been enlarged for clarity (molybdenum blue; oxygen red; carbon black; nitrogen and oxygen atoms of urea units which could not be clearly distinguished using single-crystal X-ray structure analysis, yellow). Right: interaction between polar UP-type units among themselves as well as with oxygen atoms of two hexagonal  $\{\text{Mo}_6\text{O}_6\}$  ring sites showing the (weak) potential receptor property of the cluster. The difficulty of distinguishing exactly between O and N atoms of UP is mainly caused by a  $\text{O}=\text{Mo}-\text{H}_2\text{O}$  disorder at the cluster surface (for details see ref.<sup>[20]</sup>).



work, where each individual nanocomposite acts as a “secondary building block”.

#### 4.4 Linking the {Mo<sub>154</sub>}-Type Circular Clusters to Chains

Like the [(pentagon)<sub>12</sub>(linker)<sub>30</sub>]-type nano-objects above, the {Mo<sub>154</sub>}-type wheels can also be linked to form a one-dimensional chain of the type  $\frac{1}{\infty}\{\text{Mo}_{154}\}$ . For instance, using protonated urea as a “gluing” agent it is possible to achieve such linking. The protonated urea reduces the repulsion of approaching negatively charged rings, thereby facilitating condensation between them and ultimately leading to a covalent Mo–O–Mo connectivity (see Figure 10 and ref.<sup>[20]</sup>). These findings can lead to new gateways in host-guest chemistry as the protonated urea molecules are “attached” to the nucleophilic {Mo<sub>6</sub>O<sub>6</sub>}-type “receptors” on the cluster surface [note also a new (A. Müller et al., unpublished) synthetic method for the formation of  $\frac{1}{\infty}\{\text{Mo}_{154}\}$ -type chains with “guest free” {Mo<sub>6</sub>O<sub>6</sub>} rings as well as with other cationic substrates like guanidinium].

#### 4.5 Linking the {Mo<sub>154</sub>}-Type Circular Clusters to Layers

The {Mo<sub>154</sub>}-type units are not only one-dimensionally connected to form chains but also into  $\frac{2}{\infty}\{\text{Mo}_{154}\}$ -type lay-

ers. The basic principle involves the assembly of {Mo<sub>154</sub>}-type rings as synthons by inducing a synergetically activated functional complementarity on their surface sites. The title of the corresponding paper was “*Assembling nanosized ring-shaped synthons to an anionic layer structure based on the synergetically induced functional complementarity of their surface sites*: Na<sub>21</sub>[Mo<sub>126</sub><sup>VI</sup>Mo<sub>28</sub><sup>V</sup>O<sub>462</sub>H<sub>14</sub>(H<sub>2</sub>O)<sub>54</sub>(H<sub>2</sub>PO<sub>2</sub>)<sub>7</sub>]·xH<sub>2</sub>O (x ≈ 300)”.<sup>[21]</sup> Because of the increased electron density (or nucleophilicity) of the considered Mo=O group (pointing outside of the ring), caused by the coordinated H<sub>2</sub>PO<sub>2</sub><sup>−</sup> ligand, the related ring formally acts as a ligand resulting in the substitution of the H<sub>2</sub>O ligand at a corresponding Mo=O group of another adjacent ring which has no coordinated H<sub>2</sub>PO<sub>2</sub><sup>−</sup> ligand. (Four such covalent connectivities are formed per ring.) The layered structure also leads, topologically speaking, to the formation of a system of “tubular”-type nanochannels (Figure 11). They present a possibility for the construction of a new class of materials with well-defined channel cavities (3.4 nm diameter) once the channels are freed of water and cations! Such layered networks with specific channel dimensions might be useful for size- and shape-selective reactions especially under catalytical conditions. These systems are especially attractive as they are electron rich (note: the delocalized electrons cause the blue color). It should further be mentioned that not only linking to extended structures with periodicity could be achieved but also the formation of a dimeric species.<sup>[22]</sup>

## 5. Concluding Remarks

Our investigations touched upon here are especially interesting because of the unprecedented discrete nano-objects’ properties. The spherical nanoclusters for example can be considered as “artificial cells” while they also have a strong intrinsic tendency of “responsive reactivity”.<sup>[23,24]</sup> This feature, together with the well-known catalytic properties of polyoxomolybdate clusters, could in principle lead to the emergence of a novel type of molecular catalyst and host-guest system from which functional nanodevices may evolve. One important point in this regard is the fact that several of the nano-objects (the porous capsules are, especially under O<sub>2</sub> free conditions, stable in solution) allow easy and different types of manipulations, for instance the specific affinity of the spherical capsules to cations can be “tuned” due to the modification variability of both the internal cavity shell as well as the overall charge.<sup>[31]</sup>

Although in this short voyage, various facets of covalent and noncovalent connectivity related to different states of matter have been highlighted, from “vesicular structuring” in solution via oligomeric assemblies in the gas phase to covalent connectivity in the solid state, it seems that a lot of discoveries in this context are still possible! The reason for the enormous versatility is really a consequence of the nanoscaled and especially appropriately functionalized surfaces, which resulted for instance in an interesting study to observe nucleation intermediates (title of the paper: “Kinetic Precipitation of Solution-Phase Polyoxomolybdate [...]”).

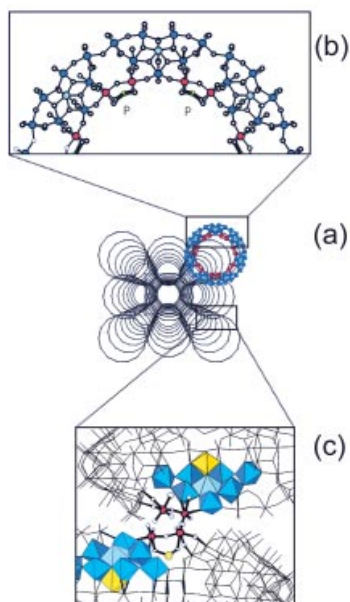


Figure 11. (a) Perspective view of the cluster framework of Na<sub>21</sub>-[Mo<sup>VI</sup><sub>126</sub>Mo<sup>V</sup><sub>28</sub>O<sub>462</sub>H<sub>14</sub>(H<sub>2</sub>O)<sub>54</sub>(H<sub>2</sub>PO<sub>2</sub>)<sub>7</sub>]·ca. 300 H<sub>2</sub>O along the crystallographic *c* axis, showing the abundance of nanotubes. For clarity, only one complete ring (without the H<sub>2</sub>PO<sub>2</sub><sup>−</sup> ligands) is shown in polyhedral representation. With respect to the other rings, only the centers of the {Mo<sub>1</sub>} units are given and connected. (b) Ball-and-stick representation of the upper half of a ring segment showing the principal positions of the H<sub>2</sub>PO<sub>2</sub><sup>−</sup> ligands. (c) Detailed view [perpendicular to (a) and (b)] of the bridging region between two cluster rings emphasizing one {Mo<sub>8</sub>}, one {Mo<sub>1</sub>} unit (in polyhedral representation) as well as one {Mo<sub>2</sub>} unit and one H<sub>2</sub>PO<sub>2</sub><sup>−</sup> ligand (without hydrogen atoms; ball-and-stick representation). The bridging (disordered) oxygen center is depicted as a large hatched circle. Colour code: {Mo<sub>2</sub>} red; {Mo<sub>8</sub>} blue (central MoO<sub>7</sub> pentagonal-bipyramid, light blue); {Mo<sub>1</sub>} yellow; P green.<sup>[21]</sup>

A Window to Solution-Phase Nanostructure").<sup>[25]</sup> An especially interesting challenge for the future will also be to place (discrete) oligomers observed in the gas phase<sup>[8]</sup> on surfaces in order to study their electronic properties.

## Acknowledgments

The authors thank Priv. Doz. Dr. D. G. Kurth and Dr. H. Bögge for their cooperation. Furthermore, financial support by the Deutsche Forschungsgemeinschaft and the Fonds der Chemischen Industrie is gratefully acknowledged. SR thanks the "Graduiertenkolleg Strukturbildungsprozesse", Universität Bielefeld, for a fellowship.

- [1] A. J. Heeger, *Angew. Chem. Int. Ed.* **2001**, *40*, 2591–2611.
- [2] a) D. Voet, J. G. Voet, *Biochemistry* 2nd ed.; Wiley: New York, **1995**; b) J.-M. Lehn, *Supramolecular Chemistry: Concepts and Perspectives*, VCH: Weinheim, **1995**; c) J. W. Steed, J. L. Atwood, *Supramolecular Chemistry*, Wiley: Chichester, **2000**; d) F. Vögtle, *Supramolecular Chemistry*, Wiley: Chichester, **1991**; e) J.-P. Behr (Ed.), *Perspectives in Supramolecular Chemistry, vol. 1: The Lock and Key Principle (The State of the Art – 100 Years On)*, Wiley: Chichester, **1994**; f) A. D. Hamilton (Ed.), *Perspectives in Supramolecular Chemistry, vol. 3: Supramolecular Control of Structure and Reactivity*, Wiley: Chichester, **1996**; g) S. Mann, *Biomaterialization: Principles and Concepts in Bioinorganic Materials Chemistry*, Oxford University Press: Oxford, **2001**; h) R. Wetherbee, *Science* **2002**, *298*, 547; i) N. Kröger, S. Lorenz, E. Brunner, M. Sumper, *Science* **2002**, *298*, 584–586; j) S. Mann, *Angew. Chem. Int. Ed.* **2000**, *39*, 3392–3406; k) S. Mann, G. A. Ozin, *Nature* **1996**, *382*, 313–318.
- [3] a) A. Müller, P. Kögerler, C. Kuhlmann, *Chem. Commun.* **1999**, 1347–1358; b) A. Müller, P. Kögerler, H. Bögge, *Structure and Bonding (Berlin)* **2000**, *96*, 203–236; c) A. Müller, F. Peters, M. T. Pope, D. Gatteschi, *Chem. Rev.* **1998**, *98*, 239–271; d) A. Müller, S. Roy, *Coord. Chem. Rev.* **2003**, *245*, 153–166; e) L. Cronin, in: (Eds.: J. A. McCleverty, T. J. Meyer), *Comprehensive Coordination Chemistry II*, Elsevier: Amsterdam, **2004**, Vol. 7, 1–56; f) A. Müller, S. Roy, in: (Eds.: C. N. R. Rao, A. Müller, A. K. Cheetham), *The Chemistry of Nanomaterials: Synthesis Properties and Applications*, Wiley-VCH: Weinheim, **2004**, pp. 452–475.
- [4] a) A. Müller, E. Krickemeyer, H. Bögge, M. Schmidtman, S. Roy, A. Berkle, *Angew. Chem. Int. Ed.* **2002**, *41*, 3604–3609, and literature cited therein; b) A. Müller, S. K. Das, S. Talismanov, S. Roy, E. Beckmann, H. Bögge, M. Schmidtman, A. Merca, A. Berkle, L. Allouche, Y. Zhou, L. Zhang, *Angew. Chem. Int. Ed.* **2003**, *42*, 5039–5044.
- [5] A. Müller, S. K. Das, E. Krickemeyer, C. Kuhlmann, *Inorg. Synth.* **2004**, *34*, 191–200.
- [6] A. Müller, E. Beckmann, H. Bögge, M. Schmidtman, A. Dress, *Angew. Chem. Int. Ed.* **2002**, *41*, 1162–1167.
- [7] a) G. Férey, *Science* **2001**, *291*, 994–995; see also: *J. Solid State Chem.* **2000**, *152*, 37–48; b) A. K. Cheetham, G. Férey, T. Loiseau, *Angew. Chem. Int. Ed.* **1999**, *38*, 3268–3292.
- [8] A. Müller, E. Diemann, S. Q. N. Shah, C. Kuhlmann, M. C. Letzel, *Chem. Commun.* **2002**, 440–441.
- [9] "Rounding up Nanoclusters: Nanotechnology", *Materials today (Research News)* **2004**, January Issue, 10.
- [10] T. Liu, E. Diemann, H. Li, A. W. M. Dress, A. Müller, *Nature* **2003**, *426*, 59–62.
- [11] The answer also came from a combination of DLS and SLS studies on the solutions containing those vesicles. The results of a DLS measurement performed on the aqueous {Mo<sub>154</sub>} solution showed that the aggregates were almost monodisperse, with an average hydrodynamic radius  $R_h$  of 45 nm. SLS data, analyzed through the Zimm plot, indicated that the average radius of gyration  $R_g$  was almost equal to the hydrodynamic radius  $R_h$ , as observed from DLS studies. It is known that for a solid spherical particle, the relationship between the two radii is  $R_g = 0.77R_h$ . If the aggregates were solid spheres with  $R_h$  around 45 nm, an  $R_g$  value of 34 nm would be expected, which was clearly not the case. As an increasing fraction of the total mass of a spherical object is distributed closer to the sphere's surface, the ratio  $R_g/R_h$  increases; the ratio approaches a value of 1 as the corresponding spherical object has all of its mass on its surface. The scattering data thus indicated that the aggregates in solution were not "solid clusters", but vesicle-like hollow spheres. (Solvents inside the spheres do not contribute to the light scattering.) Moreover the mass of the aggregates ( $M_w$ ) determined from the Zimm plot (which excludes any contained solvent) corresponded approximately to 1,165 individual nanowheels. Because a solid {Mo<sub>154</sub>}/{Mo<sub>152</sub>}-type nanocrystal with a 45 nm radius would contain more than 14,000 individual molecules, the estimated  $M_w$  value also suggested that those aggregates must have a hollow interior with 1,165 nanowheels homogeneously distributed on the surface of the vesicle.
- [12] a) A. Müller, C. Serain, *Acc. Chem. Res.* **2000**, *33*, 2–10; b) A. Oleinikova, H. Weingärtner, E. Diemann, M. Chaplin, A. Müller, (unpublished observation).
- [13] D. Volkmer, A. Du Chesne, D. G. Kurth, H. Schnablegger, P. Lehmann, M. J. Koop, A. Müller, *J. Am. Chem. Soc.* **2000**, *122*, 1995–1998.
- [14] D. G. Kurth, P. Lehmann, D. Volkmer, A. Müller, D. Schwahn, *J. Chem. Soc. Dalton Trans.* **2000**, 3989–3998.
- [15] F. A. Cotton, G. Wilkinson, C. A. Murillo, M. Bochmann, *Advanced Inorganic Chemistry*, 6th ed.; Wiley: New York, **1999**.
- [16] a) A. Müller, S. Sarkar, S. Q. N. Shah, H. Bögge, M. Schmidtman, S. Sarkar, P. Kögerler, B. Hauptfleisch, A. X. Trautwein, V. Schünemann, *Angew. Chem. Int. Ed.* **1999**, *38*, 3238–3241; b) A. Müller, E. Krickemeyer, S. K. Das, P. Kögerler, S. Sarkar, H. Bögge, M. Schmidtman, S. Sarkar, *Angew. Chem. Int. Ed.* **2000**, *39*, 1612–1614; c) A. Müller, S. K. Das, E. Krickemeyer, P. Kögerler, H. Bögge, M. Schmidtman, *Solid State Sciences* **2000**, *2*, 847–854.
- [17] A. Müller, S. K. Das, M. O. Talismanova, H. Bögge, P. Kögerler, M. Schmidtman, S. S. Talismanov, M. Luban, E. Krickemeyer, *Angew. Chem. Int. Ed.* **2002**, *41*, 579–582.
- [18] A. Müller, S. K. Das, P. Kögerler, H. Bögge, M. Schmidtman, A. X. Trautwein, V. Schünemann, E. Krickemeyer, W. Preetz, *Angew. Chem. Int. Ed.* **2000**, *39*, 3413–3417.
- [19] A. Müller, S. K. Das, H. Bögge, M. Schmidtman, A. Botar, A. Patrut, *Chem. Commun.* **2001**, 657–658.
- [20] A. Müller, S. Roy, M. Schmidtman, H. Bögge, *Chem. Commun.* **2002**, 2000–2002.
- [21] A. Müller, S. K. Das, H. Bögge, C. Beugholt, M. Schmidtman, *Chem. Commun.* **1999**, 1035–1036.
- [22] L. Cronin, C. Beugholt, E. Krickemeyer, M. Schmidtman, H. Bögge, P. Kögerler, T. K. K. Luong, A. Müller, *Angew. Chem. Int. Ed.* **2002**, *41*, 2805–2808.
- [23] A. Müller, D. Rehder, E. T. K. Haupt, A. Merca, H. Bögge, M. Schmidtman, G. Heinze-Brückner, *Angew. Chem. Int. Ed.* **2004**, *43*, 4466–4470.
- [24] A. Müller, E. Krickemeyer, H. Bögge, M. Schmidtman, S. Roy, A. Berkle, *Angew. Chem. Int. Ed.* **2002**, *41*, 3604–3609.
- [25] Y. Zhu, A. Cammers-Goodwin, B. Zhao, A. Dozier, E. C. Dickey, *Chem. Eur. J.* **2004**, *10*, 2421–2427.

Received: May 24, 2005

Published Online: August 22, 2005